CONF-850776--1

DE85 016473

CONF-850776--1

EFFECTS OF TEMPERATURE ON DISSOCIATIVE AND NONDISSOCIATIVE ELECTRON ATTACHMENT

L. G. Christophorou,* S. R. Hunter,
J. G. Carter, and S. M. Spyrou†

Atomic, Molecular and High Voltage Physics Group
Health and Safety Research Division
Oak Ridge National Laboratory
Oak Ridge, Tennessee 37831

Results of recent studies on the effects of temperature, T, on the dissociative and nondissociative electron attachment to molecules are presented and discussed. These show the delicate and large effects of T on the cross section $\sigma_{da} = \sigma_c p$ of resonance dissociative $[e + AX \underset{\tau_a^{-1}}{\overset{\sigma_c}{\rightleftharpoons}} AX^{-*} \xrightarrow{p} A + X^-]$ and $\sigma_{nd} = \sigma_c' p'$ of resonance nondissociative $[e + AX \underset{\tau_a'^{-1}}{\overset{\sigma_c'}{\rightleftharpoons}} AX^{-*} \xrightarrow{p} AX^-]$ electron attachment to a molecule AX. For AX molecules where only dissociative attachment processes occur, the effect of T on σ_{da} is an increase in σ_{da} resulting from an increase in p principally because of a decrease in the separation time of A and X^-; the energy integrated σ_{da} increases with increasing average internal energy of AX. For AX molecules with pure nondissociative attachment, the effect of T is a decrease of σ_{nd} with increasing T resulting from a decrease in p′ (i.e., an increase with T of $\tau_a'^{-1}$). For AX molecules with both dissociative and nondissociative processes the total rate constant (or cross section) increases or

---

*Also, Department of Physics, The University of Tennessee, Knoxville, Tennessee 37996.

†Present address: Theoretical and Physical Chemistry Institute, The National Hellenic Research Foundation, 48, Vassileos Constantinou Avenue, Athens 501/1, Greece.

decreases with T depending on the relative contribution of the dissociative and nondissociative processes. It appears that for both dissociative and nondissociative attachment the effect of T on σ_c or σ_c' is small except in those cases where electron capture by the hot molecule is accompanied by geometrical changes. Besides their intrinsic value, these results are of applied significance in many areas where the operating temperatures are higher than ambient and where the number density of electrons and negative ions crucially affects the performance of the device.

Introduction

Resonance electron attachment processes occur at low ($\lesssim$20 eV) energies and are generally discussed within the formalism of the resonance scattering theory and the formation of transient negative ions. Thus, resonance dissociative and nondissociative electron attachment to a molecule AX is viewed as occurring in two steps: (a) capture of the electron by AX to form the transient anion AX^{-*} and (b) the subsequent decay or stabilization of AX^{-*}; viz.,

$$e + AX \underset{\tau_a^{-1}}{\overset{\sigma_c}{\rightleftharpoons}} AX^{-*} \xrightarrow{p} A + X^- \quad \text{(dissociative)} , \qquad (1)$$

$$e + AX \underset{\tau_a'^{-1}}{\overset{\sigma_c'}{\rightleftharpoons}} AX^{-*} \xrightarrow{p'} AX^- \quad \text{(nondissociative)} . \qquad (2)$$

In reactions (1) and (2), σ_c and σ_c' are the respective electron capture cross sections, p and p' are the probabilities for AX^{-*} to decay by stable fragment [Eq. (1)] or parent [Eq. (2)] anion formation, and τ_a^{-1} and $\tau_a'^{-1}$ are the respective constants for AX^{-*} to decay by autodetachment. While many negative ion states (NISs) are usually involved in process (1), only one NIS (the lowest) is usually involved in process (2) [process (2) also requires that the electron affinity of AX is positive (>0 eV)]. In certain cases reactions (1) and (2) can proceed concomitantly and be in competition.

Processes (1) and (2) can be classified [1,2] according to the internal state of excitation of AX, viz.

$$e + AX(G;\ v \simeq 0) \xrightarrow{\sigma_c} AX^{-*}(G \text{ or } E) \Longrightarrow \text{decay} , \quad (3)$$

$$e + AX^{*}(G;\ v > 0;\ j > 0) \xrightarrow{\sigma_{c,v,j}} AX^{-*}(G \text{ or } E) \Longrightarrow \text{decay} , \quad (4)$$

$$e + AX^{*}(E) \xrightarrow{\sigma_{c,E}} AX^{-*}(E) \Longrightarrow \text{decay} . \quad (5)$$

In reaction (3), AX(G = 0, v = 0) is a molecule in its ground electronic state G and predominantly in its lowest (v = 0) vibrational state of excitation, and AX^{-*}(G or E) is the transient anion formed in either the field of the ground (G) or the field of an excited (E) electronic state with a capture cross section σ_c. In reaction (4), AX*(G = 0, v > 0, j > 0) is a molecule in its ground electronic state, but in higher vibrational (v)/rotational (j) states, and AX^{-*} (G or E) is the respective transient anion formed with a cross section $\sigma_{c,v,j}$. In reaction (5) the target molecule AX*(E) is electronically excited, and the electron is captured in the field of an excited electronic state producing AX^{-*}(E) with a cross section $\sigma_{c,E}$. Most studies to date concerned themselves with reaction (3). Swarm studies on reaction (5) are in progress at our laboratory. Electron attachment to "hot" molecules [reaction (4)] (the vibrationally/rotationally excited molecules can be formed by either laser excitation or by gas heating) have been reviewed [2].

In this paper we discuss reaction (4) with reference to published data and with reference to new results obtained at our laboratory on polyatomic halogenated compounds. Studies of the effects of temperature on the various electron attachment processes are of both intrinsic and of applied significance. With regard to the latter, in many applied areas the operating temperatures are higher than ambient and the performance of the various devices is crucially affected by the number density of electrons and negative ions (such is the case, for example, in diffuse discharge switches) and thus by T. Our discussion of resonance electron attachment to hot molecules will be separated into three parts: (a) electron attachment to molecules where only dissociative attachment processes occur, (b) electron attachment to molecules where only nondissociative electron attachment takes place, and (c) electron attachment to molecules where both dissociative and nondissociative electron attachment processes occur over an energy range.

Effects of Temperature on Electron Attachment to Molecules Where Only Dissociative Attachment Occurs

Diatomic Molecules

The cross section, σ_{da}, for (1) can be expressed as

$$\sigma_{da} = \sigma_c \, p \, . \tag{6}$$

In Eq. (6) the capture cross section σ_c depends [2-4] on the autodetachment width Γ_a and the dissociation width Γ_d and varies inversely with the resonance energy ε_{max}; the probability p is usually expressed as [2-4]

$$p = e^{-\tau_s/\tau_a} \, , \tag{7}$$

where τ_s is the average separation time of A and X^-, and τ_a is the average lifetime of AX^{-*}. As T increases, higher-lying vibrational levels of AX are populated for which the internuclear distances increase significantly (and hence the Franck-Condon region is broadened), and the magnitude of σ_{da} for molecules, AX^*_{vibr}, in such excited nuclear motion states increases significantly; also, the threshold energy is lowered, and the Γ_d is increased (e.g., see Refs. 2, 5). Such an enhancement in σ_{da}, however, can be small in cases where the dissociative attachment process is exoergic and the potential energy curve for the transient negative ion AX^{-*} crosses that of the neutral molecule close to the equilibrium separation.

The increase in σ_{da} with T results from an increase in both σ_c [as higher vibrational levels of AX are populated, progressively lower energy electrons, for which σ_c is larger [2,6], are captured (also the Franck-Condon factors change)] and p. However, the increase in σ_c is usually small [except perhaps in those cases (e.g., N_2O [7]) where geometrical changes concomitant with electron capture occur] compared with that in p; the latter dominates the T dependence of σ_{da} and results from a shortening of τ_s associated with the spatially more extended wavefunctions of AX^*_{vibr}. Theoretical calculations [2,5,8,9] have shown that the effect of rotational excitation on σ_{da} is usually small and that the effect of vibrational excitation substantially accounts for the observed increases in σ_{da} with T.

The aforementioned conclusions are based on experimental and theoretical results on diatomic molecules (O_2, H_2, D_2, HCℓ, DCℓ) [2,5,8-11]. Examples of these findings are shown in

Figs. 1 and 2. In Fig. 1 are plotted the calculated [8] values of σ_{da} close to the vertical onset for H^-/H_2 and D^-/D_2 for H_2 and D_2 in various vibrational levels v. In Fig. 2 the experimental (see figure caption) σ_{da} for $C\ell^-$ from HCℓ and DCℓ are shown for HCℓ/DCℓ in the v = 0, 1, and 2 levels. The σ_{da} increases dramatically as the vibrational quantum number increases. For a given pair of isotopic molecules, the lower the vibrational energy $h\nu_x$ of a given mode x is, the larger is the effect of T on σ_{da} since at a fixed T higher levels v_x are populated for which τ_s is shorter (p larger). It should be realized, however, that unless T is very large or ε_{max} small, the increase of the *measured* σ_{da} with T is much smaller than indicated in Figs. 1 and 2 because σ_{da} is the Boltzmann-factor-weighted σ_{da} for all levels v_x, and only a small fraction (itself a function of the size of $h\nu_x$) of molecules are in higher vibrational levels.

It has recently been pointed out [10] that the data in Figs. 1 and 2 show that the isotope effects observed [2,6] in the σ_{da} for H_2/D_2 and HCℓ/DCℓ (and for other molecules [2,6]) depend on T. As T increases, τ_s decreases and hence the isotope effects become less pronounced; for a given T, higher vibrational levels (for which p is larger) are populated in the heavier molecule ($h\nu_D < h\nu_H$) and thus the increase in σ_{da} with T is larger for the heavier than for the lighter analog (see insets in Figs. 1 and 2). Actually (see inset in Fig. 2), when HCℓ/DCℓ have vibrational energy $\gtrsim$0.1 eV this increase in σ_{da} overtakes the opposite effect (decrease) introduced by the larger reduced mass of D-$C\ell^-$ compared with H-$C\ell^-$, so that the ratio $[\sigma_{da}(\varepsilon_{max})]_{DC\ell}/[\sigma_{da}(\varepsilon_{max})]_{HC\ell}$ which for HCℓ and DCℓ in the v = 0 level is equal to 0.71 (Ref. 12) becomes >1.

The cross section data for the various v levels of H_2 and D_2 in Fig. 1 have been used [10] to determine the contributions to the total $\sigma_{da}(T)$ from the various vibrational levels at a number of T; at each value of T the cross section for a particular vibrational level v (see Fig. 1) was multiplied by the fractional population of that level. The resultant cross sections $\sigma_{da}(v)$ are shown in Fig. 3 along with the total $\sigma_{da}(T)$ [the sum of $\sigma_{da}(v)$ over all contributing v levels]. Although these results are approximate (the cross sections in Fig. 1 for the various v are threshold values [8]), it is clear that as T increases the isotope effect decreases (see inset in Fig. 3).

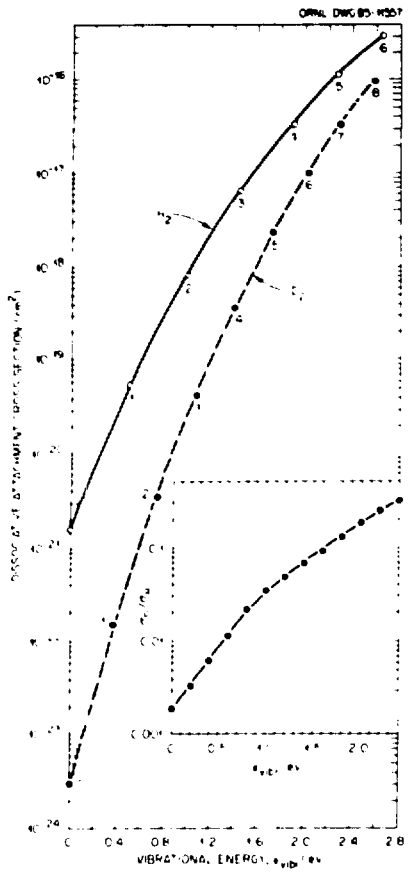

Figure 1. Calculated [8] σ_{da} for H^-/H_2 and D^-/D_2 with H_2/D_2 in various vibrational levels. The data are for energies close to the vertical onset. Inset: Ratio σ_D/σ_H of the σ_{da} for D^-/D_2 and H^-/H_2 as a function of the neutral molecule's vibrational energy (from Ref. 10).

Similar calculations [10] for HCℓ and DCℓ are more limited since for these molecules only cross section data for the v = 0, 1, and 2 levels are available (see Fig. 2) and the effect of rotational excitation of $\sigma_{da}(T)$ may not be insignificant [9,11] as was the case for H_2 and D_2 [8,14]. Nevertheless, the contributions to the total dissociative attachment cross section $\sigma_{da}(T)$ from the v = 0, 1, and 2 vibrational levels in Fig. 4 show that the total $\sigma_{da}(T)$ of DCℓ exceeds that of HCℓ at $T \gtrsim 650$ K (see inset in Fig. 4), while it is only 70% that of HCℓ at $T \simeq 300$ K.

It is thus apparent [10] that the isotope effects observed in dissociative attachment depend on gas temperature; they are

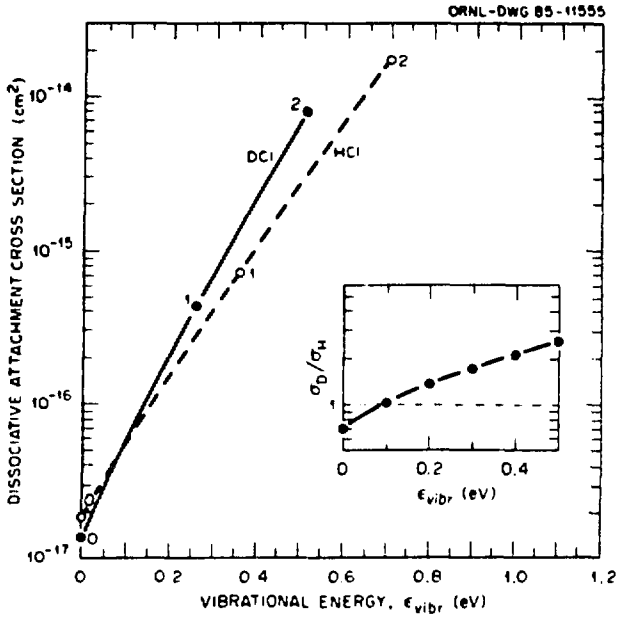

Figure 2. Experimental [11] σ_{da} for $C\ell^-$/HCℓ and $C\ell^-$/DCℓ for HCℓ and DCℓ in the v = 0, 1, and 2 levels. These cross sections were obtained from the values reported in Ref. 11 for the ratios $\sigma_{da}(v = 1,2)/\sigma_{da}(v = 0)$ for HCℓ and DCℓ [$\sigma_{da}(v = 1)/\sigma_{da}(v = 0)$ and $\sigma_{da}(v = 2)/\sigma_{da}(v = 0)$ were reported [11] to be, respectively, 38 and 880 for HCℓ and 32 and 580 for DCℓ] and by normalizing the $\sigma_{da}(v = 0)$ relative cross section of Ref. 11 to the cross section measured [12] at T ≃ 300 K (the peak value of σ_{da} for HCℓ and DCℓ is, respectively, equal to 1.95 and 1.4 $\times 10^{-17}$ cm^2 at ∿0.8 eV [12]) (from Ref. 10).

the largest when the isotopic molecules are in their v = 0 levels. It is also apparent that while for diatomic molecules the ratio $\sigma_{da}(v > 0)/\sigma_{da}(v = 0)$ increases with increasing vibrational energy, for a given T the internal energy is a function of the magnitude of $h\nu_x$ and for polyatomic molecules also of the number of vibrational degrees of freedom N.

Polyatomic Molecules

Earlier work on the effect of T on σ_{da} of polyatomic molecules has been reviewed [2]. Recent work on freons, which are of interest as additives in multicomponent gas mixtures for use as gaseous dielectrics or in diffuse discharge switches, has been undertaken at our laboratory, and some of the results we obtained are presented and discussed in this and the following sections.

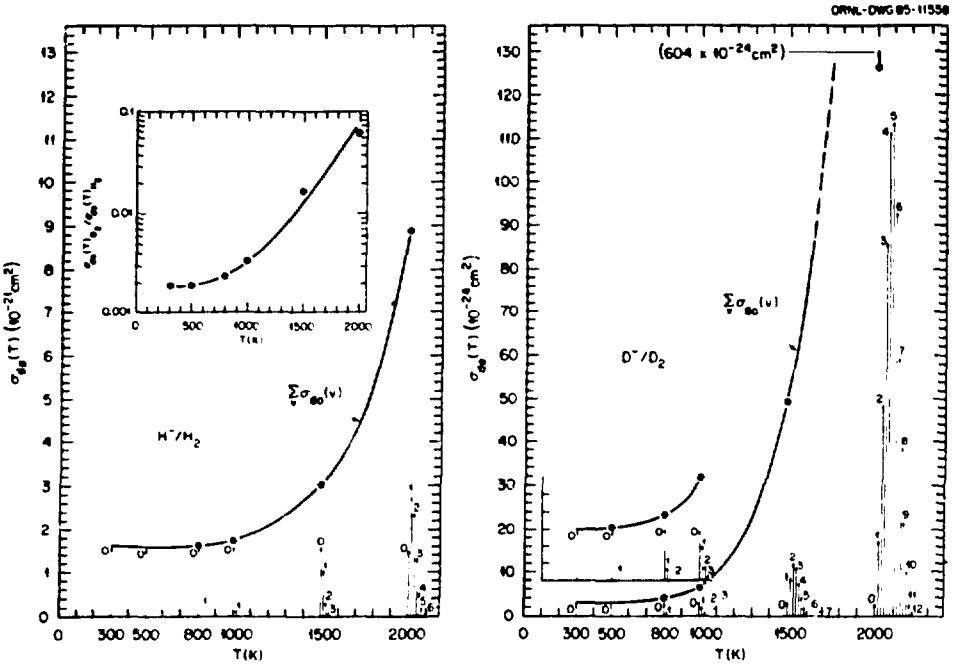

Figure 3. Dissociative attachment cross section $\sigma_{da}(T)$ for H^-/H_2 and D^-/D_2 at various T determined as described in the text. For each T the length of the vertical arrows designated by 0,1,2...gives the contribution $\sigma_{da}(v)$ to the total $\sigma_{da}(T) = \Sigma_v \sigma_{da}(v)$ of molecules, respectively, in the v = 0,1,2...levels. The energy, E_v, of the v = 0,1,2...vibrational levels was determined using the formula $E_v = hc\omega_e(v + \frac{1}{2}) - hc\omega_e\chi_e(v + \frac{1}{2})^2$, where h is the Planck constant, c is the speed of light, and ω_e and $\omega_e\chi_e$ are the vibrational constants given in Ref. 13. As T increases, progressively larger contributions to $\sigma_{da}(T)$ come from molecules in higher vibrational quantum states. Inset: Ratio $\sigma_{da}(T)_{D_2}/\sigma_{da}(T)_{H_2}$ at various T (from Ref. 10).

$CC\ell F_3$. In Fig. 5 are given the measured [15] total electron attachment rate constants $k_a(\langle\varepsilon\rangle)$ as a function of the mean electron energy $\langle\varepsilon\rangle$ for $300 \leq T \leq 700$ K. As T increases, k_a increases, especially at low $\langle\varepsilon\rangle$. In Fig. 6 are shown the total electron attachment cross sections $\sigma_a(\varepsilon)$ obtained [15] at each value of T from the respective $k_a(\langle\varepsilon\rangle,T)$ in Fig. 5 via the swarm unfolding technique [16]. The peak at ~1.5 eV is especially sensitive to changes in T. The peak value of $\sigma_a(\varepsilon)$ is increased by a factor of 3, and the energy position, ε_{max}, of the peak and the energy onset, A0, shift progressively to lower energy as T increases. Electron beam studies (inset,

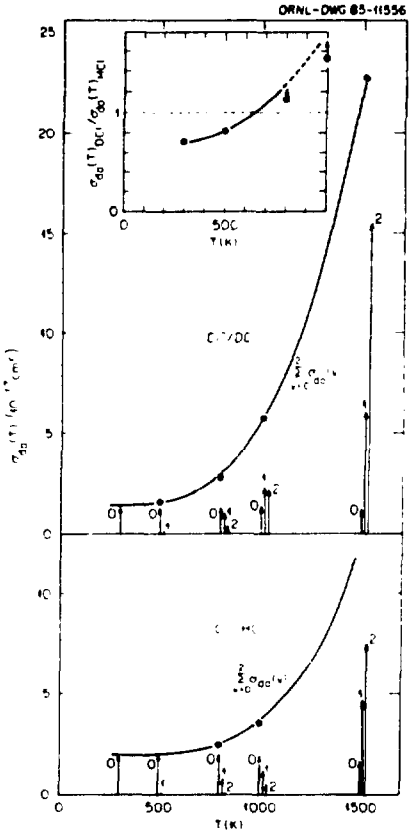

Figure 4. Dissociative attachment cross section $\sigma_{da}(T)$ for $C\ell^-/HC\ell$ and $C\ell^-/DC\ell$ at various T determined as described in the text. For each T the length of the vertical arrows designated by 0, 1, and 2 gives the contribution $\sigma_{da}(v)$ to the total $\sigma_{da}(T)$ of molecules, respectively, in the $v = 0$, 1, and 2 vibrational levels (the energy of each vibrational level was determined as described in the caption of Fig. 3). The sum, $\sum_{v=0}^{2} \sigma_{da}(v)$, of the $\sigma_{da}(v)$ for the v = 0, 1, and 2 levels is also given in the figure. Since for T ≥ 1000 K the contributions to $\sigma_{da}(T)$ of molecules in $v > 2$ is substantial, the values of $\sigma_{da}(T)$ [$\equiv \sum_{v=0}^{2} \sigma_{da}(v)$] in the figure for 1000 and 1500 K are grossly underestimated. As a consequence of this, the values of the ratio $[\sigma_{da}(T)]_{DC\ell}/[\sigma_{da}(T)]_{HC\ell}$ for 1000 and 1500 K (see inset) are lower than their true values (this is indicated in the inset by the data points ↑) (from Ref. 10).

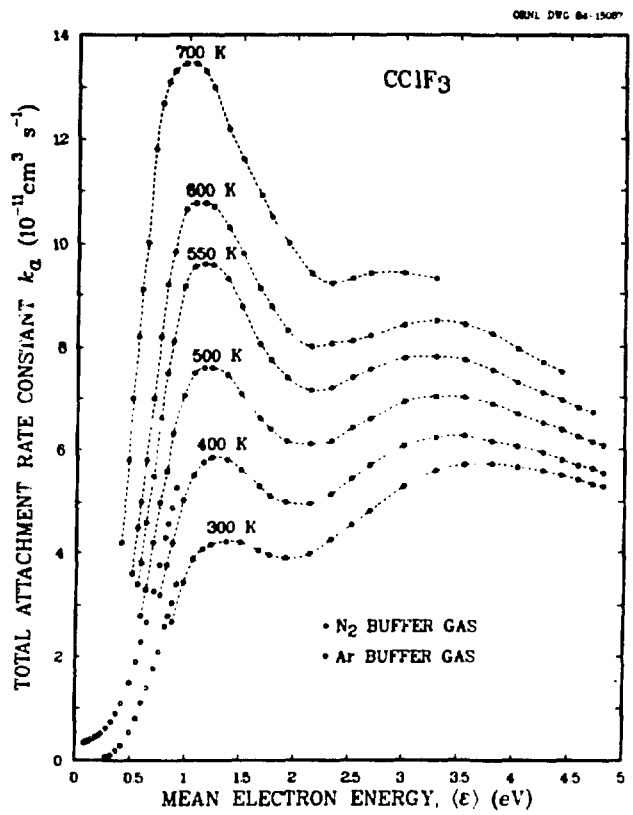

Figure 5. Total electron attachment cross section versus electron energy for $CC\ell F_3$ measured [15] in the buffer gases N_2 or Ar at various temperatures; the $k_a(\langle\varepsilon\rangle)$ were independent of gas number density.

Fig. 6) have shown [15] that at low gas pressures $CC\ell F_3$ captures electrons exclusively via dissociative attachment and that the peaks at ∿1.5 and ∿4.7 eV are the former due to $C\ell^-$ and the latter due to $C\ell^-$, F^-, $CC\ell F_2^-$, and $C\ell F^-$ ions.

C_2F_6. In Fig. 7 the $k_a(\langle\varepsilon\rangle,T)$ are given along with the relative abundance of the fragment negative ions observed (inset, Fig. 7) in a beam study [17]. No parent negative ions were observed in the low pressure beam study, and this is consistent with the absence of any pressure dependence of $k_a(\langle\varepsilon\rangle,T)$ in the swarm study. In Fig. 8 are plotted the swarm unfolded cross sections which show a single peak due to F^- and CF_3^- (see inset of Fig. 7). The decrease in ε_{max} and AO and the increase in FWHM (full width at half maximum) of $\sigma_a(\varepsilon)$ with T are shown in the inset of Fig. 8.

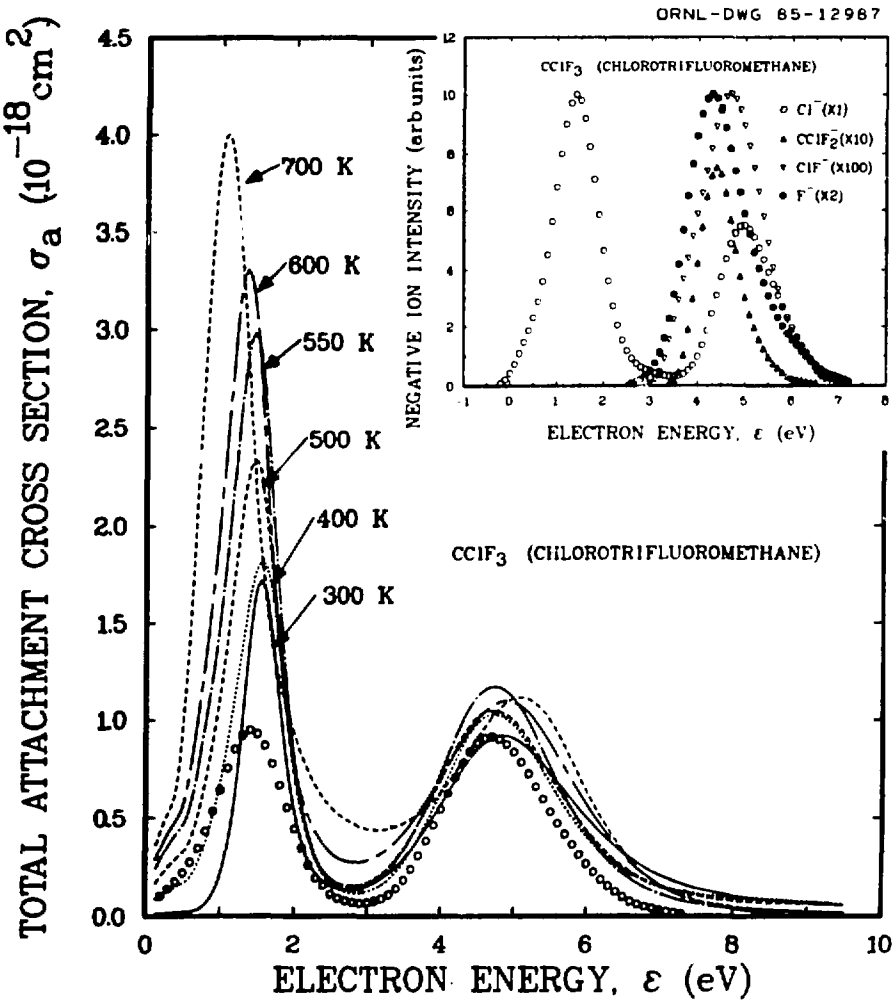

Figure 6. Total electron attachment cross section versus electron energy for $CC\ell F_3$ unfolded from the $k_a(\langle\varepsilon\rangle,T)$ data in Fig. 5 at various T. The curve designated by the open circles (o) is the electron beam total attachment cross section normalized to the high energy peak of the swarm unfolded cross section for 300 K. Inset: Relative intensity of the dissociative attachment negative ions produced by low energy electron impact on $CC\ell F_3$ as a function of electron energy measured in a beam study (these spectra were corrected for the finite width of the electron pulse) [15].

In addition to the $k_a(\langle\varepsilon\rangle),T)$ we measured in mixtures with Ar, we also measured the electron attachment, $\eta/N_a(E/N)$, and ionization, $\alpha/N_a(E/N)$, coefficients in pure C_2F_6 at 300 and

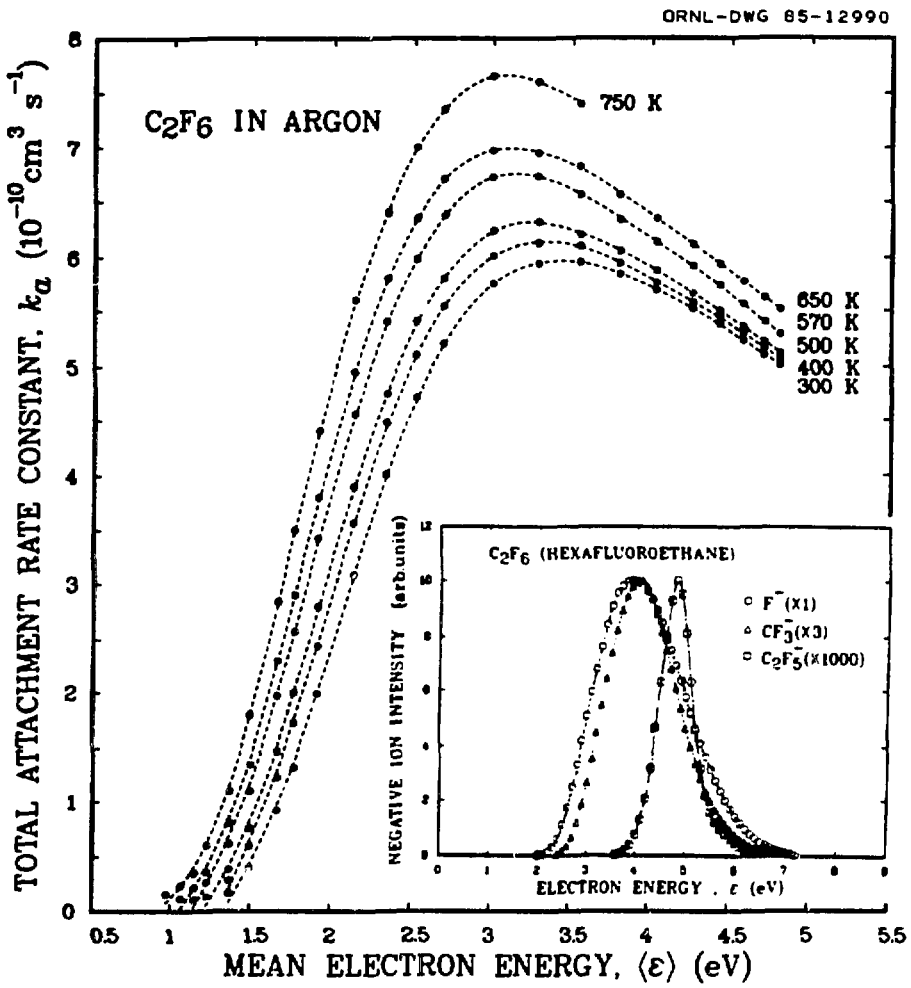

Figure 7. Total electron attachment rate constant as a function of mean electron energy for C_2F_6 in Ar buffer gas at various temperatures. The $k_a(\langle\varepsilon\rangle,T)$ were independent of gas number density [15]. Inset: Relative intensity of the dissociative attachment fragment anions measured [17] in a low pressure beam study.

500 K. These measurements are shown in Fig. 9. The η/N_a data are consistent with those obtained in mixtures of C_2F_6 with Ar (Fig. 7).

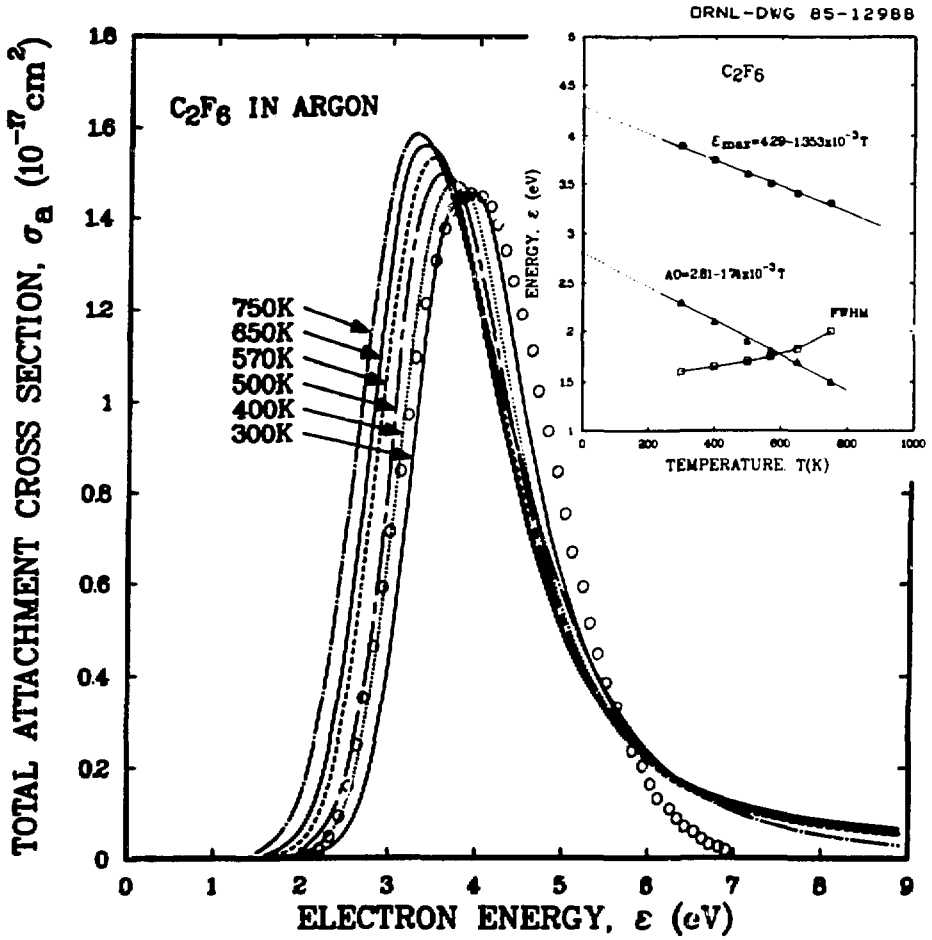

Figure 8. Total electron attachment cross section versus electron energy unfolded from the $k_a(\langle\varepsilon\rangle,T)$ data in Fig. 7 at the indicated temperatures. The open circles (o) are the total electron beam cross section normalized to the peak of the swarm unfolded cross section for 300 K. Inset: Variation of the cross section peak position (ε_{max}), cross section onset energy (AO), and cross section full width at half maximum (FWHM) with temperature (from Ref. 15).

Variation of the Energy Integrated Attachment Cross Section with Temperature and with the Molecule's Internal Energy

We have determined the energy integrated attachment cross section

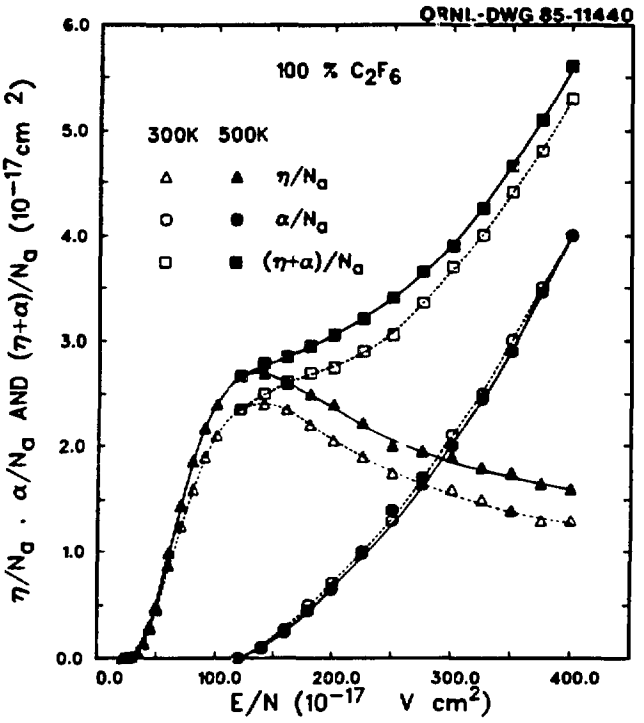

Figure 9. Electron attachment, η/N_a, and ionization, α/N_a, coefficients and their sum, $(\eta + \alpha)/N_a$, as a function of E/N at 300 and 500 K for pure C_2F_6.

$$\int_{\varepsilon_{min}}^{\varepsilon_{max}} \sigma_{da}(\varepsilon,T)\, d\varepsilon \equiv \sigma_{EIA}(T) \qquad (8)$$

from the respective $\sigma_{da}(\varepsilon,T)$ measured for O^-/O_2 [18], $C\ell^-/HC\ell$ [11,19], $C\ell^-/CC\ell F_3$ [15], O^-/N_2O [7,20], SF_5^-/SF_6 [22,23], C_2F_6 [15] (all ions), and C_3F_8 [26] (all ions). These are plotted in Fig. 10a. The σ_{EIA} increases with T; this increase varies from molecule to molecule but not, however, in the simple fashion (i.e., the lower the σ_{EIA} at T = 300 K the faster its increase with T) stated earlier [27].

The fast increase of σ_{EIA} with T for SF_5^-/SF_6 and O^-/N_2O is most interesting. For SF_6 this may be due to the larger increase in p with increasing T probably because almost all 15 vibrational frequencies of SF_6 are small [774 cm^{-1} (singly degenerate); 642 cm^{-1} (doubly degenerate); 948, 616, 525, and 347 cm^{-1} (all triply degenerate)] [28] and hence high-lying levels of each mode are populated at relatively low T; also, it should be noted that the ε_{max} for SF_5^-/SF_6 is low (~0.37 eV

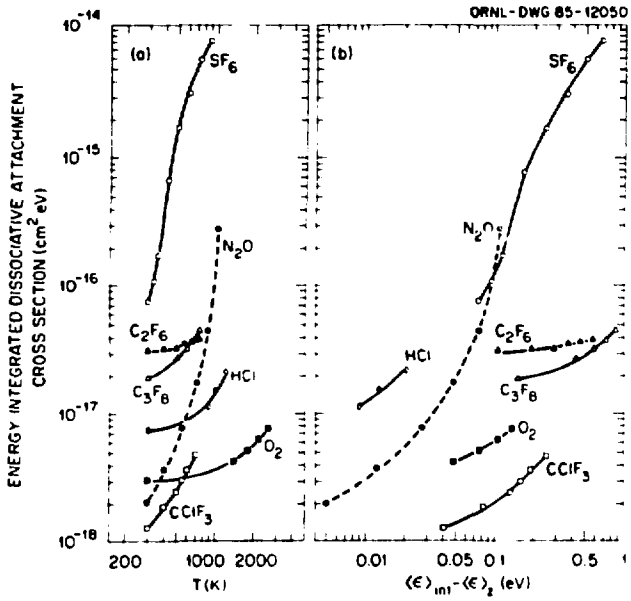

Figure 10. Energy integrated dissociative attachment cross section as a function of temperature (Fig. 10a) and excess internal energy $\langle\varepsilon\rangle_{int}-\langle\varepsilon\rangle_z$ (Fig. 10b) for O_2, $HC\ell$, N_2O, SF_6, $CC\ell F_3$, C_2F_6, and C_3F_8 (see the text).

[24]) and that all six SF_5-F coordinates lead to SF_5^-. For N_2O the large increase of σ_{EIA} with T may result from the fact that as T increases the hot N_2O^* molecule (in the bending mode) [7,29] better facilitates upon electron collision the geometrical changes (from a straight N_2O^* to a bend N_2O^{-*}) which are known to occur concomitantly with electron capture. It has been suggested [7] that the increased excitation in the bending mode of N_2O results in a lowering of the position of the NIS which leads to O^- formation; this would increase greatly the magnitude of σ_c and, thus, σ_{da}.

At any T there is a Boltzmann distribution B_v of the population of the vibrational levels v of each vibrational mode x. For a molecule with N normal modes, the vibrational energies of the normal mode x in the v = 0,1,2,....levels (if we neglect anharmonicity) are $\varepsilon_{v,x} = (v + \frac{1}{2})h\nu_x$ and for each x

$$B_v = e^{-\varepsilon_v/kT} / \sum_{v=0}^{\infty} e^{-\varepsilon_v/kT} . \qquad (9)$$

If we neglect the effect of rotational excitation and consider only the effect of vibrational excitation to be significant,

then for a diatomic molecule the cross section $\sigma_{da}(\varepsilon,T)$ can be expressed as

$$\sigma_{da}(\varepsilon,T) = \sum_{v=0}^{\infty} B_v \sigma_{da}^{v}(\varepsilon,T) \ . \qquad (10)$$

For a polyatomic molecule the summation in (10) must be carried out for all x. However, even if this were possible the x are not independent.

Let us then assume that as T increases each vibrational mode x of a polyatomic molecule is excited by an equal probability and that the total average internal energy $\langle\varepsilon\rangle_{int}$ of the molecule is principally the sum of the energy in the various normal modes, x, viz.

$$\langle\varepsilon\rangle_{int} = \sum_{x=1}^{N} \sum_{v=0}^{\infty} D_x B_v \varepsilon_{v,x} \ , \qquad (11)$$

where D_x is the degeneracy of the mode x. If we take $\langle\varepsilon\rangle_{int}$ to be the molecule's *total* internal energy, then the molecule's excess energy would be $\langle\varepsilon\rangle_{int}-\langle\varepsilon\rangle_z$, where $\langle\varepsilon\rangle_z$ ($\equiv \sum_{x=1}^{N} \frac{1}{2} h\nu_x$) is the zero-point energy. If now, $\langle\varepsilon\rangle_{int}-\langle\varepsilon\rangle_z$ is distributed quickly among the molecule's N vibrational degrees of freedom and can thus become available for the dissociative attachment reaction, one might expect a relationship between σ_{EIA} and $\langle\varepsilon\rangle_{int}-\langle\varepsilon\rangle_z$. Indeed, σ_{EIA} increases with $\langle\varepsilon\rangle_{int}-\langle\varepsilon\rangle_z$ (see Fig. 10b), although this increase differs--as expected--from one molecule to another. Actually, a better comparison might have been a plot of σ_{EIA} versus $(\langle\varepsilon\rangle_{int}-\langle\varepsilon\rangle_z)/\varepsilon_{max}$. This would shift the C_2F_6, C_3F_8, O_2, and $CC\ell F_3$ curves to lower energies compared with SF_6 for which ε_{max} = 0.37 eV. The fact that the curves in Fig. 10b for SF_6 and N_2O mesh reasonably well although ε_{max} for SF_6 is 0.37 eV and for N_2O it is 2.25 eV is consistent with the arguments presented earlier in this section that the ε_{max} for electron attachment to N_2O^* (bending mode) is lower than the ε_{max} for electron attachment to unexcited N_2O.

While further experimental and theoretical work is necessary (especially on polyatomic molecules) to fully understand the effect of temperature on $\sigma_{da}(\varepsilon)$ and $\sigma_{EIA}(T)$, it is clear that for both diatomic and polyatomic molecules the changes in $k_{da}(\langle\varepsilon\rangle)$, $\sigma_{da}(\varepsilon)$, and $\sigma_{EIA}(T)$ with T result principally from an increase with T of the internal energy ($\simeq$ vibrational) of the molecule.

Effect of Temperature on Nondissociative Electron Attachment

The cross section, σ_{nd}, for nondissociative electron attachment--as that, σ_{da}, for dissociative varies profoundly with the gas temperature. Based on the data outlined in this section, this dependence arises from an effect of T on both σ_c' and p'. However, while for dissociative attachment σ_{da} generally *increases* with T, for nondissociative attachment σ_{nd} generally *decreases* with T. Furthermore, while in dissociative attachment the increase in σ_{da} with T is predominantly due to a decrease in τ_s (and thus increase in p), the decrease in σ_{nd} for nondissociative attachment is due to a decrease in τ_a (and thus decrease in p) and σ_c'. These conclusions are based on the following results.

SF_6

The cross section for the formation of SF_5^- from SF_6 at ~0.0 eV has been found to increase dramatically with increasing T (Fig. 10; Refs. 2, 22). However, a number of studies [2] have shown that the total attachment cross section or rate constant for SF_6 is independent of T to ~1200 K. This implies that the formation of SF_6^- (whose σ_{nd} peaks at ~0.0 eV [2]) decreases with increasing T. Direct evidence for this is provided by the early work of Hickam and Berg [30]. It is presently not possible to which quantity, σ_c' or p', to ascribe this decrease in σ_{nd} with T, although p is expected to decrease with increasing T because τ_a is expected to decrease as the internal energy of SF_6^{-*} increases [2,6].

1-C_3F_6

A large decrease of the attachment rate constant for nondissociative electron attachment to perfluoropropylene (1-C_3F_6) with increasing T has been observed (Fig. 11; Refs. 2, 31, 32). This has been attributed [31,32] to a decrease in the τ_a of 1-$C_3F_6^{-*}$ with increasing T.

C_6F_6

A profound decrease in the rate constant for electron attachment to perfluorobenzene (C_6F_6) with T has been reported for C_6F_6 (Fig. 12; Ref. 33). At T = 300 K, C_6F_6 forms parent $C_6F_6^-$ ions by capturing near-zero energy electrons [2]; the τ_a of $C_6F_6^{-*}$ was found to be ~10 μs [2]. Spyrou and Christophorou [33] concluded that the decrease in $k_a(\langle\varepsilon\rangle)$ with T (Fig. 12) cannot be attributed to a decrease in τ_a (decrease in p) with T [the $k_a(\langle\varepsilon\rangle)$ did not depend on the gas number

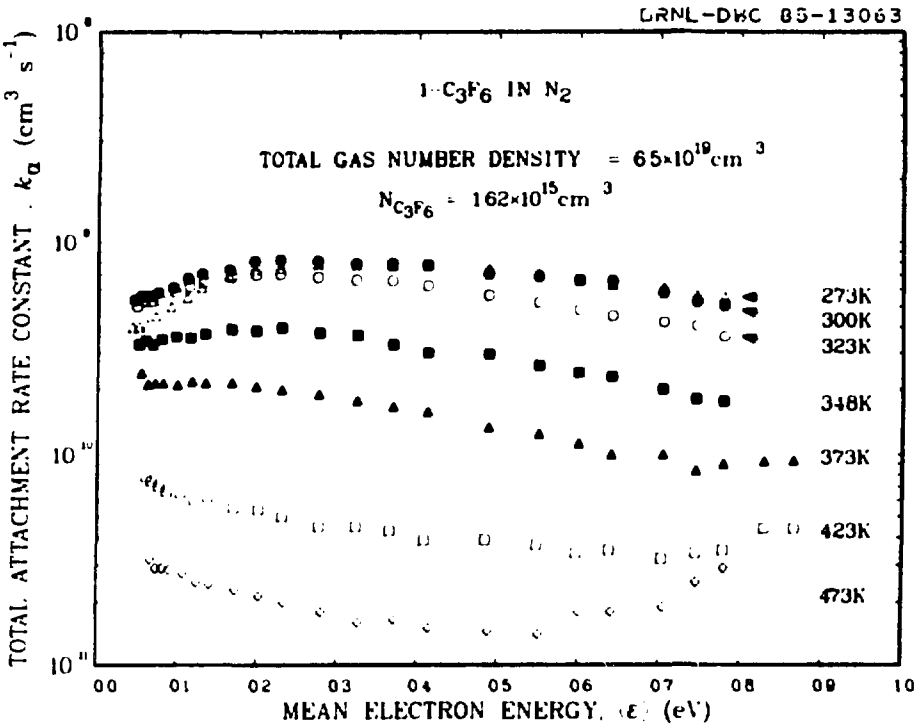

Figure 11. Total attachment rate constant versus mean electron energy for 1-C_3F_6 in N_2 at 273 ≤ T ≤ 473 K (from Ref. 32).

density at any T] or other by-products resulting from gas heating. They attributed it to a decrease in σ_c' and suggested that the increase in the internal energy of C_6F_6 affects rather profoundly the rate for the capture transition (i.e., to differences in the magnitude of σ_c' for the reactions e + $C_6F_6 \rightarrow C_6F_6^{-*}$ and e + $C_6F_6^* \rightarrow C_6F_6^{-*}$).

While much improvement in our understanding of the effects of the internal energy of a molecule on its electron attachment properties is still desirable, it is clear that as a rule σ_{da} increases and σ_{nd} decreases with increasing internal energy, that is, increasing T. It is also apparent that for both dissociative and nondissociative electron attachment p is the determining factor unless geometrical changes concomitant with electron capture effect changes in σ_c or σ_c'.

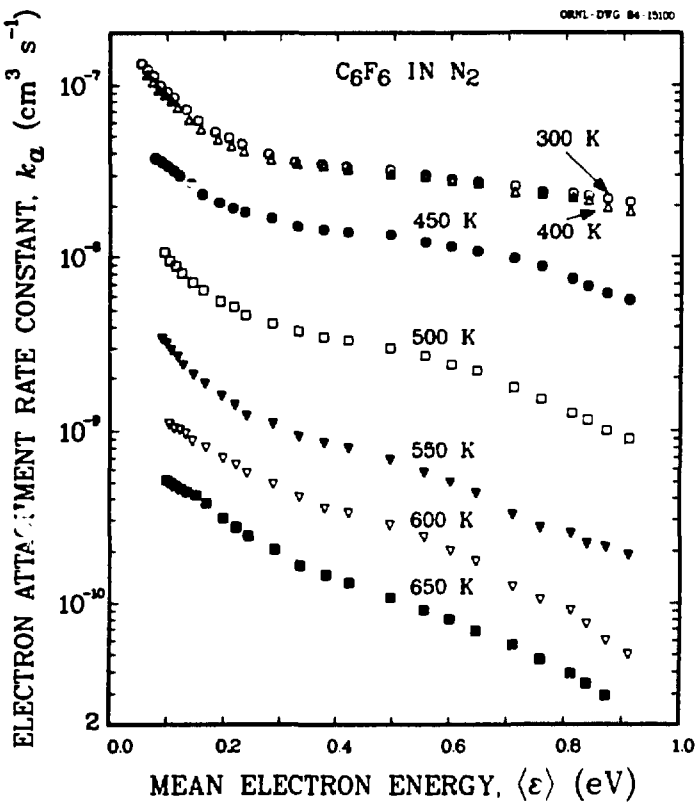

Figure 12. $k_a(\langle\varepsilon\rangle,T)$ for C_6F_6 measured in a buffer gas of N_2. The C_6F_6 gas number density varied from 0.41 to 46.3 × 10^{13} cm^{-3} and that of N_2 from 2.25 to 6.44 × 10^{19} cm^{-3} (from Ref. 33).

Effect of Temperature on the Measured Attachment Rate Constant and Cross Section for Molecules for Which Both Dissociative and Nondissociative Electron Attachment Occur Over an Energy Range

Recently, we measured [26] the total electron attachment rate constant $k_a(\langle\varepsilon\rangle)$ for C_3F_8 in Ar in the temperature range from 300 to 750 K. At $T \lesssim 425$ K the $k_a(\langle\varepsilon\rangle)$ were found to increase with increasing total gas number density N_t over the entire $\langle\varepsilon\rangle$ range (∿0.5 to ∿5 eV) covered in these experiments. At 450 K, the $k_a(\langle\varepsilon\rangle)$ increased with N_t only for $\langle\varepsilon\rangle \lesssim 1.2$ eV and at $T > 450$ K the $k_a(\langle\varepsilon\rangle)$ were independent of N_t. The $k_a(\langle\varepsilon\rangle)$ also showed a weak dependence on the attaching gas number density N_a due to the effect of the presence of the attaching gas on the distribution functions of pure Ar used in

the analysis; this effect was taken into account by measuring, for a fixed N_t, the $k_a(\langle\varepsilon\rangle)$ as a function of N_a and extrapolating at each $\langle\varepsilon\rangle$ the $k_a(N_a)$ to $N_a \rightarrow 0$.

In Fig. 13 are plotted the values, $k_1(\langle\varepsilon\rangle)$, of $k_a(\langle\varepsilon\rangle)$ for $N_a \rightarrow 0$ and $N_t \rightarrow 0$ for all values of T that data were taken, and in Fig. 14 k_1 is plotted as a function of T for two values of $\langle\varepsilon\rangle$. It is evident from these data that $k_1(\langle\varepsilon\rangle)$ decreases to a minimum around 450 to 500 K and that it then increases as T increases.

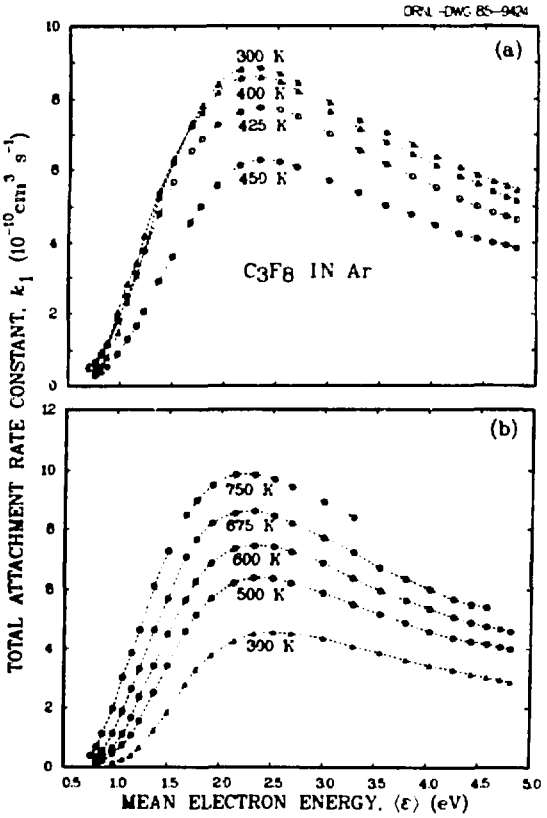

Figure 13. Electron attachment rate constant k_1 ($N_a \rightarrow 0$; $N_t \rightarrow \infty$) for C_3F_8 measured as a function of mean electron energy $\langle\varepsilon\rangle$ in a buffer gas of Ar at (a) 300, 400, 425, and 450 K and (b) 500, 600, 675, and 750 K. The 300 K curve in Fig. 13b is the dissociative attachment contribution to the measured $k_a(\langle\varepsilon\rangle)$ at this temperature (see the text and Ref. 26).

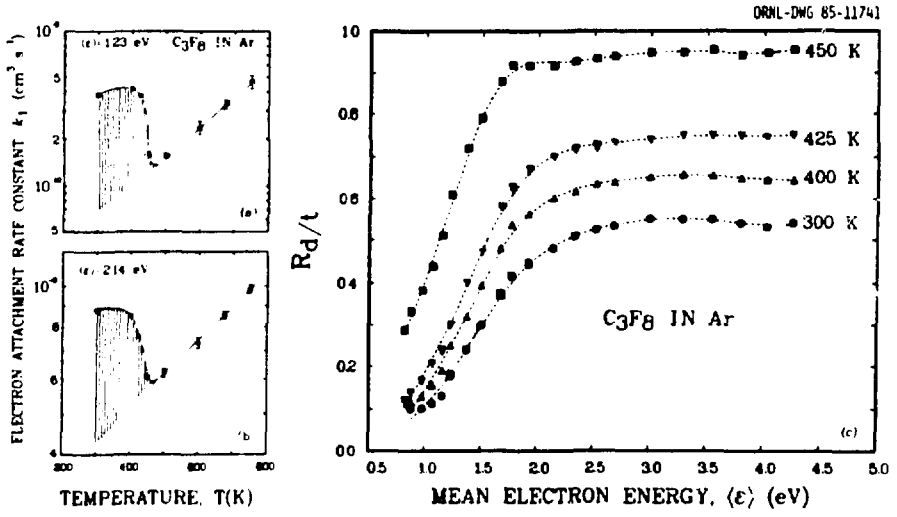

Figure 14. (a) and (b) Electron attachment rate constant k_1 ($N_a \to 0$; $N_t \to \infty$) for C_3F_8 versus temperature T at the mean electron energies $\langle\varepsilon\rangle$ = 1.23 and 2.14 eV. (c) Ratio $R_{d/t}$ of the attachment rate constant due to dissociative attachment to the total attachment rate constant (see the text) versus the mean electron energy at 300, 400, 425, and 450 K obtained from extrapolation of the $k_a(\langle\varepsilon\rangle)$ measured at T ≥ 500 K to lower T (see the text).

The delicate dependence of $k_a(\langle\varepsilon\rangle)$ on T can be understood by considering the results of electron beam and electron swarm studies. Single collision beam experiments on C_3F_8 indicated the presence of only dissociative attachment anions and established their identity and energy dependence; they also showed the existence of a number of NISs which lead to dissociative attachment [17]. On the other hand, the results of high pressure swarm experiments on C_3F_8 determined the magnitude of the total attachment rate constant and cross section as a function of electron energy and their total pressure dependence [26,34]; they indicated that in addition to the NISs which lead to dissociative attachment (observed in single collision beam experiments) there exists another, lower-lying NIS which is attractive and which leads to the formation of parent negative ions with $\tau_a < 10^{-6}$ s [26,34]. These findings and the observed effects of T on $k_a(\langle\varepsilon\rangle)$ (Figs. 13 and 14) and $\sigma_{da}(\varepsilon)$ (Fig. 15) have been ascribed to electron attachment via an attractive NIS (with a positive electron affinity and a steep repulsive part) leading to parent anions and to one (or more) repulsive NISs leading to fragment anions.

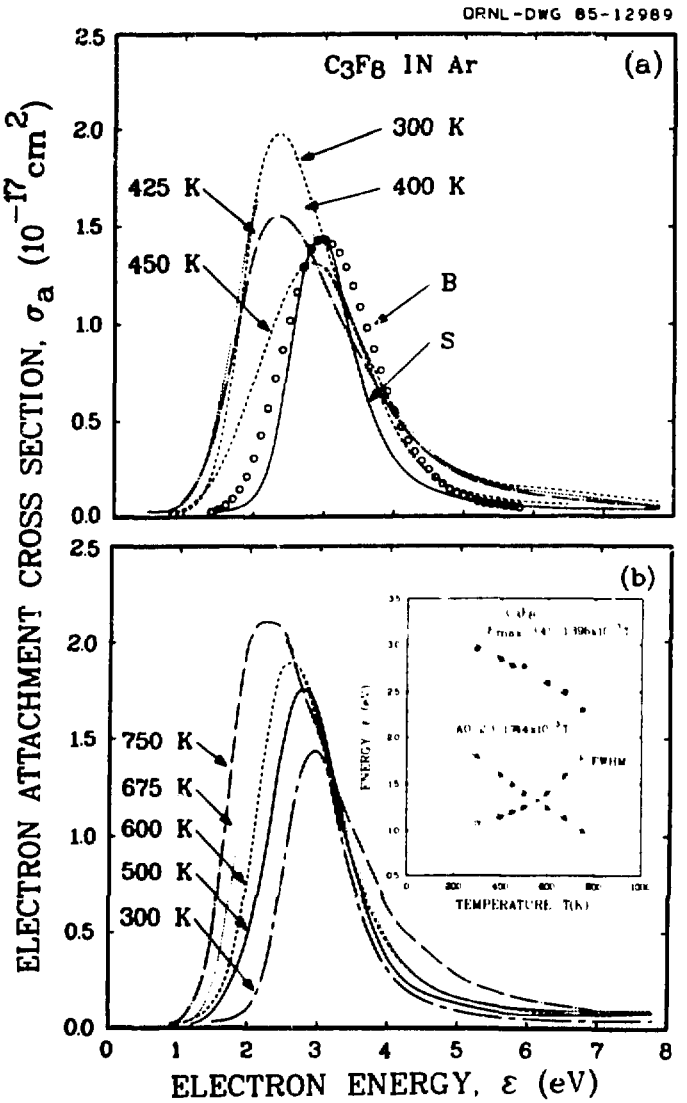

Figure 15. Swarm unfolded *total* electron attachment cross section $\sigma_a(\varepsilon)$ for C_3F_8 obtained [26] from the $k_1(\langle\varepsilon\rangle)$ in Ar shown in Fig. 13 at (a) 300, 400, 425, and 450 K and (b) 300, 500, 600, 675, and 750 K. In Fig. 15a is plotted also the *dissociative* attachment cross section $\sigma_{da}(\varepsilon)$ obtained from the swarm data at 300 K (curve S) and the dissociative cross section measured in an electron beam experiment (curve B) which has been normalized to the peak of $\sigma_{da}(\varepsilon)$ (see the text). In Fig. 15b the curve for 300 K is the curve S of Fig. 15a. Inset: Variation of peak energy (ε_{max}), appearance onset (AO), and full width at half maximum (FWHM) of the total dissociative attachment cross section of C_3F_8 with temperature.

The delicate dependence of $k_a(\langle\varepsilon\rangle)$ on T (Figs. 13 and 14) can thus be considered as the result of two opposite effects of T: one on the rate constant for nondissociative and the other on the rate constant for dissociative electron attachment. As it has been shown in the previous section, as a rule, the rate constant for pure nondissociative attachment processes decreases and that for pure dissociative attachment processes increases with increasing T. At each $\langle\varepsilon\rangle$, the magnitude of k_a is determined by the relative magnitudes of the rate constants for nondissociative and dissociative electron attachment both of which depend on T. From the data in Fig. 14, it is apparent that for $T \gtrsim 500$ K the principal contribution to the measured k_a originates from dissociative attachment; this is supported by the lack of any dependence of k_a on N_t at high T and from the observed increases in k_a with T^a (500 to 750 K) which are characteristic of molecules which attach electrons dissociatively. We then assumed [26] that for $T \gtrsim 500$ K the measured k_a is due entirely to dissociative attachment and extrapolated (at various values of $\langle\varepsilon\rangle$) the measured k_a at $T \gtrsim 500$ K to lower T (see Figs. 14a,b) in an effort to estimate the dissociative attachment contribution to the measured k_a at $T \lesssim 500$ K, where nondissociative attachment takes place and becomes progressively more significant with decreasing T. From plots such as those in Figs. 14a,b we estimated [26] the ratio $R_{d/t}(\langle\varepsilon\rangle)$ of the dissociative to the total attachment rate constant as a function of $\langle\varepsilon\rangle$ for 300, 400, 425, and 450 K. These estimates are given in Fig. 14c and show that the contribution of dissociative attachment processes to the measured rate constant is both a function of $\langle\varepsilon\rangle$ and T.

The total electron attachment rate constants $k_1(\langle\varepsilon\rangle)$ (Fig. 13) were unfolded [26] and the total attachment cross sections $\sigma_a(\varepsilon,T)$ obtained are shown in Fig. 15. They decrease in magnitude with increasing T from 300 to ~450 K (Fig. 15a) because in this T range the total cross section contains a large contribution (which decreases as T increases) from *nondissociative* attachment. An increase in T beyond ~450 K (Fig. 15b) results in an overall increase in the magnitude and full width at half maximum--and a shift to lower energy of the onset and energy of the peak (see inset of Fig. 15b)--resulting from the increasingly larger contribution of the *dissociative* attachment component to the total cross section.

In Fig. 15a are also compared the cross sections due to only the dissociative attachment contribution to the total cross section at 300 K (curve S) and the total (for all fragment anions) dissociative attachment cross section for C_3F_8 measured in a single collision electron beam study [17];

the latter was normalized to the peak value of the former. It is seen that the peak positions of the two cross section functions agree well and that both lie at a higher energy than the total unfolded cross section $\sigma_a(\varepsilon,300\ K)$.

Conclusions

While much improvement in our understanding of the effects of internal energy of a molecule on its electron attaching properties is still desirable, it is clear that as a rule σ_{da} increases and σ_{nd} decreases with increasing T. It is also apparent from the data obtained to date that for both dissociative and nondissociative electron attachment the survival probability is the determining factor (shortening of τ_s in dissociative and shortening of τ_a in nondissociative electron attachment with increasing T) unless geometrical changes concomitant with electron capture effect changes in $\sigma_c(\sigma_c')$.

From the practical point of view, both the increases and the decreases in $k_a(\langle\varepsilon\rangle)$ with T are significant because they affect the conductivity/dielectric strength properties of the gaseous medium. The sensitivity of $k_a(\langle\varepsilon\rangle)$ to changes in T requires that proper attention be given to the operating temperature range of a given device. Interestingly, the sensitivity of $k_a(\langle\varepsilon\rangle)$ to T (e.g., C_6F_6; see Fig. 12) can perhaps be employed to change the conducting/insulating properties of a gaseous medium by varying T.

Acknowledgments

Research sponsored in part by the Office of Health and Environmental Research, U.S. Department of Energy, under contract DE-AC05-840R21400 and in part by the Office of Naval Research under interagency agreement 43 01 24 60 2 with Martin Marietta Energy Systems, Inc.

References

[1] Christophorou, L. G. *Environ. Health Perspect.* 1980, 36, 3.

[2] Christophorou, L. G.; McCorkle, D. L.; Christodoulides, A. A. In "Electron-Molecule Interactions and Their Applications"; Christophorou, L. G., Ed.; Academic Press: New York, 1984; Volume 1, Chapter 6.

[3] O'Malley, T. F. Phys. Rev. 1966, 150, 14.
[4] Bardsley, J. N.; Herzenberg, A.; Mandl, F. Proc. Phys. Soc. (London) 1966, 89, 321.
[5] O'Malley, T. F. Phys. Rev. 1967, 155, 59.
[6] Christophorou, L. G. "Atomic and Molecular Radiation Physics"; Wiley-Interscience: New York, 1971; Chapter 6.
[7] Chantry, P. J. J. Chem. Phys. 1969, 51, 3369.
[8] Bardsley, J. N.; Wadehra, J. M. Phys. Rev. 1979, 20, 1398.
[9] Bardsley, J. N.; Wadehra, J. M. J. Chem. Phys. 1983, 78, 7227.
[10] Christophorou, L. G. J. Chem. Phys. (submitted).
[11] Allan, M; Wong, S. F. J. Chem. Phys. 1981, 74, 1687.
[12] Christophorou, L. G.; Compton, R. N.; Dickson, H. W. J. Chem. Phys. 1968, 48, 1949.
[13] Huber, K. P.; Herzberg, G. "Molecular Spectra and Molecular Structure. IV. Constants of Diatomic Molecules", Van Nostrand Reinhold Company: New York, 1979.
[14] Allan, M.; Wong, S. F. Phys. Rev. Lett. 1978, 41, 1791.
[15] Spyrou, S. M.; Christophorou, L. G. J. Chem. Phys. 1985, 82, 2620.
[16] Christophorou, L. G.; McCorkle, D. L.; Anderson, V. E. J. Phys. B 1971, 4, 1163.
[17] Spyrou, S. M.; Sauers, I.; Christophorou, L. G. J. Chem. Phys. 1983, 78, 7200.
[18] For O_2 we used the calculated values of O'Malley [5] which fitted well the experimental results.
[19] These cross sections were obtained using the relative cross section data of Ref. 11 at various T and by normalizing these to the room temperature cross section values of Ref. 12.
[20] These cross sections were obtained using the relative cross section data of Ref. 7 at various T and normalizing the room temperature intensity at 2.3 eV to 8.3×10^{-18} cm^2 [21].
[21] Chaney, E. L.; Christophorou, L. G. J. Chem. Phys. 1969, 51, 883.
[22] Chen, C. L.; Chantry, P. J. J. Chem. Phys. 1979, 71, 3897.
[23] The cross sections at various T were obtained using the relative cross section of Ref. 22 and taking for the cross section maximum for SF_5^-/SF_6^- at 0.37 eV [24] the value [25] of 9.8×10^{-16} cm^2. Since in the time-of-flight studies of Ref. 24 the temperature was higher (~350 K) than ambient (due to heating of the collision chamber by the filament), it was assumed that the 9.8×10^{-16} cm^2 value corresponds to $T \simeq 355$ K.

[24] Christophorou, L. G.; McCorkle, D. L.; Carter, J. G. J. Chem. Phys. 1971, 54, 253.
[25] Christophorou, L. G.; McCorkle, D. L.; Carter, J. G. J. Chem. Phys. 1972, 57, 2228.
[26] Spyrou, S. M.; Christophorou, L. G. J. Chem. Phys. (in press).
[27] Spence, D; Schulz, G. J. J. Chem. Phys. 1973, 58, 1800.
[28] Shimanouchi, T. NSRDS-NBS 39, June 1972.
[29] N_2O has three normal modes: NN stretch (2224 cm^{-1}), bend (589 cm^{-1}), and NO stretch (1285 cm^{-1}) [28].
[30] Hickam, W. M.; Berg, D. J. Chem. Phys. 1958, 29, 517.
[31] Hunter, S. R.; Christophorou, L. G.; McCorkle, D. L.; Sauers, I; Ellis, H. W.; James, D. R. J. Phys. D 1980, 16, 573.
[32] McCorkle, D. L.; Christophorou, L. G.; Hunter, S. R. In "Proceedings of the Third International Swarm Seminar"; Lindinger, W.; Villinger, H.; Federer, W., Eds.; Innsbruck, Austria, 1933; p. 37.
[33] Spyrou, S. M.; Christophorou, L. G. J. Chem. Phys. 1985, 82, 1048.
[34] Hunter, S. R.; Christophorou, L. G. J. Chem. Phys. 1984, 80, 6150.